Subtle variations in the structure of crosslinked epoxy networks and the impact upon mechanical and thermal properties

AUTHOR(S)

Larry Reyes, Jane Zhang, B Dao, D L Nguyen, Russell Varley

PUBLICATION DATE

05-08-2020

HANDLE

10536/DRO/DU:30134285

JOURNAL OF Applied Polymer SCIENCE

Subtle variations in the structure of crosslinked epoxy networks and the impact upon mechanical and thermal properties

Larry Q. Reyes,[1] Jane Zhang,[1] Buu Dao,[2] Duc L. Nguyen,[1] Russell J. Varley[1]

[1]Carbon Nexus at the Institute for Frontier Materials, Deakin University, Waurn Ponds, Victoria 3216, Australia

[2]CSIRO Manufacturing, Bag 10, Clayton MDC, Victoria 3169, Australia

Correspondence to: R. J. Varley (E-mail: russell.varley@deakin.edu.au)

ABSTRACT: Presented here is an investigation of the structure–property relationships of crosslinked networks using three bi-functional glycidyl ether aromatic epoxy resins, two bi-aryl and one tri-aryl, cured with bi- and tri-aryl amines. Subtle changes to the monomer chemistry including changing aromatic substitution patterns from meta to para, methylene to isopropyl and isopropyl to ether were explored. Changing an epoxy resin backbone from methylene to isopropyl enhances backbone rigidity thus increasing glass transition temperature (T_g), yield strength, and strain despite reducing modulus. Changing meta-substitution to para increases T_g and yield strain while leaving strength unaffected and reducing modulus. Changing isopropyl linkages to ether reduces modulus, strength, T_g, and yield strain reflecting increased molecular flexibility. Using three instead of two aromatic rings increases the molecular weight between crosslinks thereby decreasing T_g and yield strain while increasing modulus and strength. Despite the complexities of multiple systems for varying epoxy resins and amine hardeners, the effect upon network properties is explained in terms of short- and long-range molecular and segmental mobility, crosslink density, and equilibrium packing density. © 2020 Wiley Periodicals, Inc. J. Appl. Polym. Sci. **2020**, *137*, 48874.

KEYWORDS: crosslinking; kinetics; structure-property relationships; thermosets

Received 11 September 2019; accepted 15 December 2019

DOI: 10.1002/app.48874

INTRODUCTION

Since the discovery of epoxy resins in the 1940s, they have found widespread usage across an enormous number of applications in adhesives, sealants, coatings, insulators, and composites, in every imaginable manufacturing industry.[1–3] Their benefits are many, and well known, including excellent mechanical properties and corrosion, thermal and chemical resistance to name a few.[1,4–6] Another important advantage is their comparative ease of processability, such as low viscosity, long pot life and importantly little to no evolution of volatiles during cure.[7,8] However, another major factor that has continued to aid their proliferation throughout various industries is the enormous range of available monomers of varying structure, viscosity, and reactivity.[9–13] This has enabled formulators and resin chemists to continuously refine and modify resin systems with specific properties tailored to the intended application. However, much of this formulating is based upon practical experience and know-how, rather than a fundamental understanding of the structure–property relationships in crosslinked epoxy–amine networks. The purpose of this article, therefore, is to expound on the effect of systematically varying some subtle structural features of an epoxy resin or an amine hardener on the properties of the cured network. In this way, the insights gained may provide guidance to the development of new resin formulations for fine control of properties.

Structure–property processing relationships in common epoxy–amine networks are generally well established with respect to variables such as aliphatic versus aromatic moieties,[14–16] crosslink density,[17–19]and substituent effects.[17,20–22] For example, increasing aromaticity in a polymer network increases thermal stability and mechanical properties, while likely reducing processability through increased viscosity and reduced reactivity. Similarly, increasing crosslink density increases the glass transition temperature,[18,19] stiffness,[17,23] and strength,[17,24–26] but tends to make the network more brittle and susceptible to impact damage. Finally, substituent effects[21,22,27–29] whether through steric hindrances, resonance effects, and electronic inductive effects are known to impact reactivity and hence final properties of the network. However, more subtle structure–property relationships are also critically important, as small changes in a network have been shown to have large effects on the final network. A common example of this is the difference in reactivity and final properties arising from varying the substitution in diamino diphenyl sulfone (DDS) from meta to para (i.e., 33 DDS to 44 DDS). Changing substitution from meta to para significantly increases T_g and yield

strain while reducing modulus and can be attributed to anti-plasticization reducing equilibrium packing density. A recent study by Ramsdale-Cooper and Foreman found some similar trends in meta to para substitution in common epoxy–amine resin systems but additionally reported that fracture toughness was only improved for networks based upon meta-substituted amines and not epoxy resins.[17] Indeed, Vogel *et al.* have complemented these findings for various substituted isomers of tri-aryl ether amines and reported a profound yet systematic impact upon reactivity, glass transition temperature, and mechanical properties.[21]

This article, therefore, focuses on much less studied subtle variations in structure and the resultant impact upon mechanical and thermal properties of the fully cured network. Three commercially available and relatively common epoxy resins were used, diglycidyl ether of bisphenol A (DGEBA), diglycidyl ether of bisphenol F (DGEBF), and diglycidyl ether of bisphenol M (DGEBM), and cured with four different amine hardeners. DGEBA and DGEBF differ only in the central linkage between the two aryl groups, DGEBA containing a central isopropyl group while DGEBF a methylene group. The DGEBM differs from DGEBA in that it is a tri-aryl epoxy resin consisting of two meta-substituted isopropyl groups linking a central aromatic ring with para-substituted outer aromatic rings. The amine hardeners used were methylene dianiline (MDA), 1,4 bis(4-isopropyl aniline) benzene (BisPA), 1,3 bis(4-isopropyl aniline) benzene, (BisMA), and 1,3-bis(4-aminophenoxy) benzene (TPE-R). The MDA acts as a bi-aryl benchmark from which other tri-aryl amines are compared. The BisPA and BisMA contain two isopropyl linkages differing only by their substitution of the central aromatic ring. TPE-R consists of ether linkages instead of isopropyl groups and is centrally meta substituted similar to BisMA. In summary, therefore, the structural variations explored here are

- methylene versus isopropyl groups of the epoxy,
- bi- versus tri-aryl rings in the epoxy and amine,
- meta versus para isopropyl substitution of the central aromatic ring, and
- ether versus isopropyl substitution of the meta-substituted central aromatic ring.

The chemical structures are shown in Figure 1. The 12 formulations were fully cured and the polymer networks were characterized using near-infrared spectroscopy, compressive properties, thermal properties [dynamic mechanical and thermomechanical analysis and differential scanning calorimetry (DSC)], and solvent resistance. Through these studies, the development of new epoxy resin systems for applications in the aerospace, wind energy, automotive and construction industries requiring no additional modification will be enabled.

EXPERIMENTAL

Materials

The epoxy resins used were diglycidyl ether of bisphenol A referred to as DGEBA (DER331, The Dow Chemical Company, Australia, EEW 189 g/eq.), diglycidyl ether of bisphenol F referred as DGEBF (GY285, Hunstman Advanced Materials, Australia, EEW 168 g/eq.), and 1,3 bis(4-isopropyl phenyl glycidyl ether) benzene referred to as DGEBM (Solvay, Longview, WA, EEW 229 g/eq.). The amines used were MDA (Sigma-Aldrich, Australia, AEW 49 g/eq.), BisPA, Chriskev, Lenexa, KS, AEW 86 g/eq.), BisMA (Chriskev, AEW 86 g/eq.), and TPE-R (Hunstman Advanced Technologies Australia, AEW 73 g/eq.). The amines were all powders while the epoxy resins were viscous liquids. All chemicals were used as received, though prior to blending and curing, they were all degassed under vacuum at 80 °C overnight.

Sample Preparation

Each epoxy–amine formulation was prepared according to the following general procedure. The epoxy resin was further degassed at 100 °C on a rotary evaporator under vacuum at about 120 °C and −100 kPa for 1 h. The hardener was then added slowly to the epoxy such that the overall stoichiometry was 1:1 epoxide:amino groups and mixing continued until the hardener had dissolved into the epoxy resin and was free of bubbles. The resin was then poured into preheated Teflon-coated molds and cured at 150 °C for 2 h, 177 °C for 4 h, and finally 205 °C for 2 h.

Characterization

Thermal Analysis. Dynamic mechanical thermal analysis (DMTA) was performed using a Perkin-Elmer SEIKO DMA Diamond II Series. Samples of dimensions 12 × 50 × 2.8 mm^3 were placed in a dual cantilever fixture using a force amplitude of 20 μm at a frequency of 1 Hz. The glass transition temperature (T_g) of the network was determined from the peak in the tan δ spectra after a temperature ramp from 50 to 250 °C at a rate of 2 °C min^{-1}. The glassy and rubbery moduli were measured at 50 and 50 °C above the T_g, respectively. From the theory of rubbery elasticity, the crosslink density (ν_e) of the network was determined from the value of the rubbery modulus E_r at T_r (T_g + 50 °C)

$$\nu_e = \frac{E_r}{3RT_r}$$

DSC was performed using a Mettler DSC821^e DSC in the dynamic mode by placing 10 mg of the resin in an aluminum crucible inside the furnace under a blanket of nitrogen at a constant flow rate of 50 mL min^{-1}. The resin was then heated from 50 to 300 °C at a rate of 10 °C min^{-1} to determine the T_g of the network and also to establish if the network was completely cured. The temperature range over which the T_g occurred was measured by taking the difference between the onset and offset temperature of the glass transition ($\Delta T = T_{offset} - T_{onset}$).

The coefficients of thermal expansion (CTE) of the networks were determined using a TA Thermomechanical Analyser Q400 and following the test method ASTM E831. Samples were machined into dimensions 5 × 5 × 2 mm^3 (length × width × thickness) using a diamond saw. An expansion quartz probe, with an initial applied force of 10 mN, determined the dimensional changes from 25 to 250 °C at a heating rate of 5 °C min^{-1} and nitrogen gas purging of 50 mL min^{-1}. Glassy CTE were derived between 25 and 100 °C using the following equation:

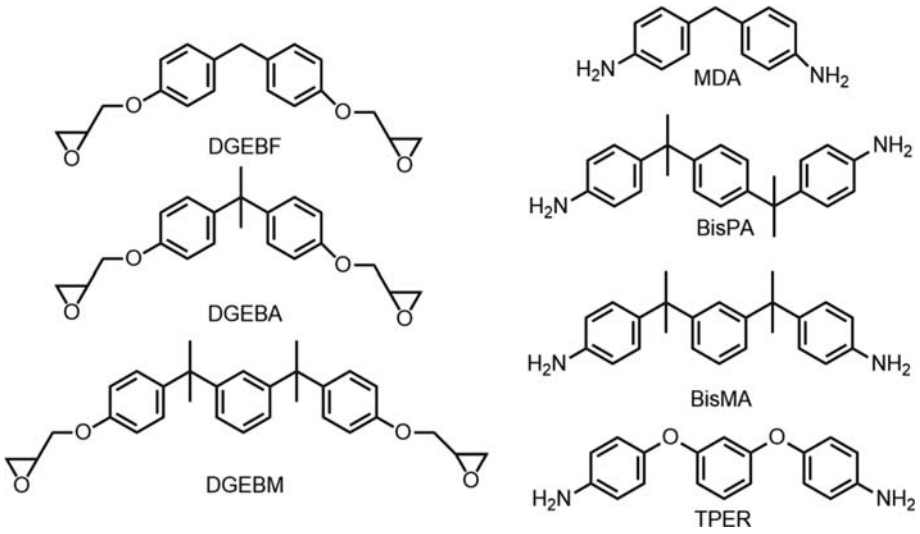

Figure 1. Chemical structures of epoxy resins and amine hardeners.

$$\alpha = \frac{1}{L}\frac{\Delta L}{\Delta T} \quad (1)$$

where L is the initial length of the specimen at 25 °C, ΔL is the difference of the length of the specimen at 100 °C (T2) and 25 °C (T1) and ΔT is the difference between T2 and T1.

Compressive properties were determined using an Instron 3880 Universal Testing Machine fitted with a 100 kN load cell and flat platens. Cylindrical samples of approximately 12 mm in height and a diameter of 12 mm were placed between the platens and compressed using a crosshead displacement of 1 mm min^{-1}.

Near-infrared (NIR) analysis was determined using a Bruker Alpha Fourier-Transform Infrared Spectrometer. The samples were placed inside the universal sampling module and measurements were made between 4000 and 7000 cm^{-1} in transmission using a resolution of 4 cm^{-1} and an average of 64 scans.

Methyl ethyl ketone (MEK) ingress was determined by placing cured resin cylinders, with dimensions of 15 × 15 mm^2 (diameter × height) and mass of around 3 g, in a 50 mL Schott bottles containing 40 mL of MEK. The bottles were sealed and were incubated at 25 °C for 1, 4, 8, 11, 15, 18, 22, 28, 29 days.

$$\%\text{change in mass} = \frac{m_t - m_i}{m_i} \times 100\%$$

where m_t is the mass at the collection time and m_i is the initial mass. The change in mass was determined in triplicate.

RESULTS AND DISCUSSION

Network Formation

Epoxy–amine cure is initiated through primary amine addition to the strained three-membered oxirane group increasing molecular weight and modestly increasing the glass transition temperature (T_g).[20] The depletion of the primary amine coincides with gelation, the incipient formation of a 3D single macromolecular network, beyond which it is no longer completely soluble. Gelation occurs at a defined epoxide conversion dependent controlled by the functionality of the amine and epoxide reactants according to the Flory–Stockmayer's equation as follows:

$$\alpha_{gel}^2 = \frac{1}{(f_e - 1)(f_a - 1)}$$

where α_{gel} is the cure conversion at the gel point, and the f_e and f_a are the functionalities of the epoxy and amine, respectively.[30] Given that each of the resin systems has the same epoxy and amine functionality, the gelation is theoretically the same at 58% epoxide conversion. Beyond gelation, the secondary amine groups are consumed as continued nucleophilic addition to the oxirane groups cause crosslinking and a rapid increase in mechanical and thermal properties. As the T_g of the network approaches the cure temperature, vitrification drastically reduces molecular mobility transforming the mechanism from being chemically controlled to diffusion controlled. At this point, side reactions such as internal cyclization and homopolymerization begin to compete with secondary amine addition.[21,29] Given the potential disparity between the epoxide conversion, reaction kinetics, and mechanism, it is necessary to characterize the network structure to ensure that any differences can be attributed to structure rather than incomplete cure, unreacted functional groups, or variations in the cure mechanism.

NIR spectroscopy is an ideal technique to characterize this network since the epoxide, primary and secondary amine, and hydroxyl groups all have strong and distinct peaks in the 4000–7000 cm^{-1} range. Figure 2(a) shows NIR spectra for the DGEBA networks cured with each amine, and the lack of any significant epoxide peak at about 4570 cm^{-1} suggests extremely high epoxide consumption. Although the primary amine peak at 4700 cm^{-1} is completely depleted as expected, a strong hydroxyl peak at just under 7000 cm^{-1} and a weak secondary amine peak at about 6640 cm^{-1} are present. The hydroxyl peak is evidence of nucleophilic addition to the epoxide groups, while the very low

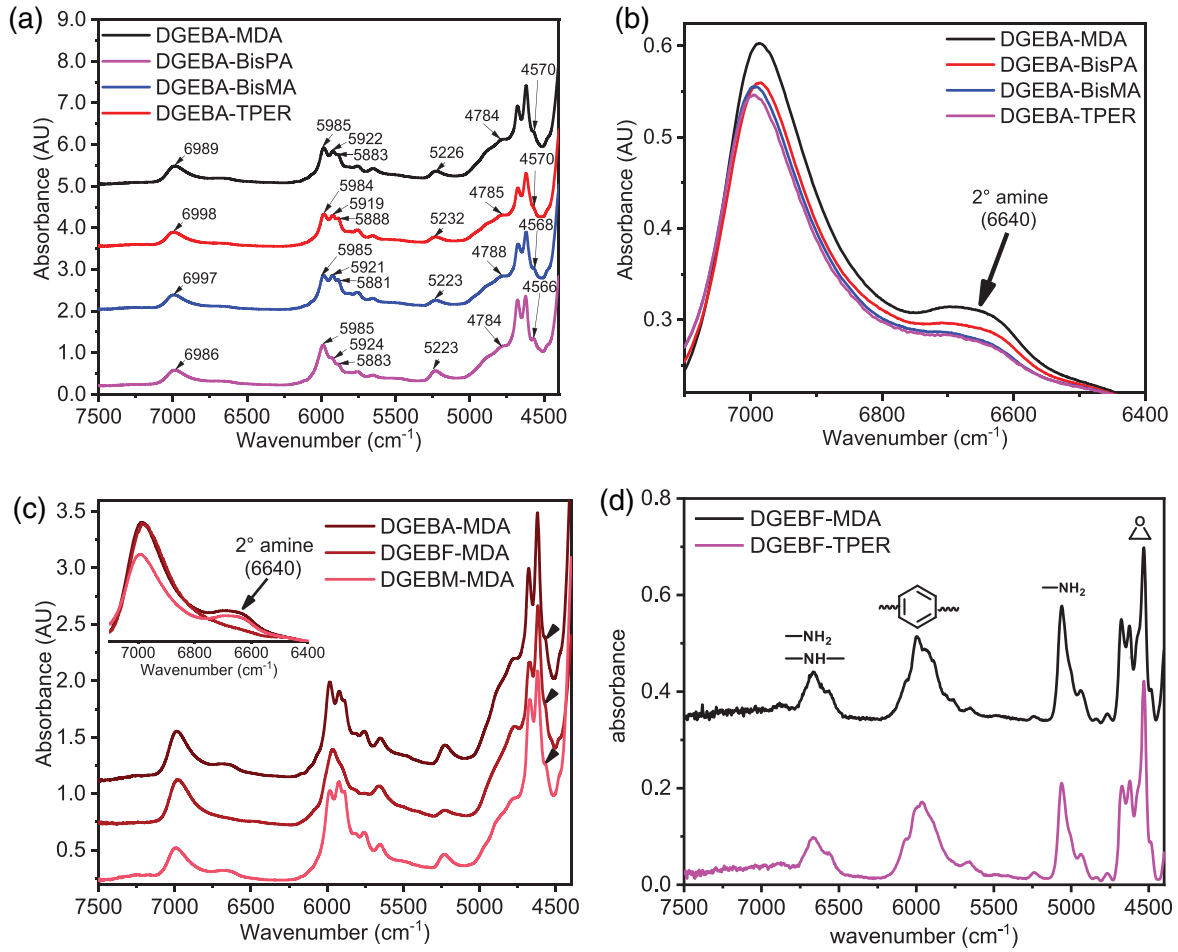

Figure 2. Near-infrared spectra of the cured epoxy–amine networks showing (a) the effect of the different amines using DGEBA, (b) an expanded view of the hydroxyl and secondary amine region for the DGEBA cured networks, (c) the effect of the different epoxy resins cured with MDA and d) the DGEBF/MDA and DGEBF/TPER resin systems prior to cure. The inset expands the view of the hydroxyl and secondary amine region. [Color figure can be viewed at wileyonlinelibrary.com]

intensity and diffuse secondary amine peak is indirect evidence again for very high levels of epoxide cure. An expanded view of this region in Figure 2(b) suggests the different amines have little impact on the DGEBA-based networks. Similar results were found for the DGEBF and DGEBM networks, although for the DGEBF network, no secondary amine peak was observed at all indicating even higher secondary amine conversion for the methylene linked epoxy resin as shown in Figure 2(c). It is surmised then that the methylene linkage, para to the reactive oxirane group is still able to impart higher reactivity to the epoxy resin compared with the isopropyl-linked DGEBA and DGEBM resins. Furthermore, Figure 2(d) shows two examples of uncured resin systems, DGEBF/MDA and DGEBF/TPER, to illustrate the presence of the epoxide and primary amine groups prior to cure. The large epoxide peak at 4570 cm^{-1} and the primary amine peaks at 4700 cm^{-1} at about 6640 cm-1 are all consumed during cure and for this reason, the peak at 6640 cm^{-1} after cure can be attributed solely to secondary amine groups in the cured network. It is important to note that the peak at about 6000 cm^{-1} is attributed to phenyl group vibrations of the epoxy backbone, which act as a kind of internal standard enabling qualitative evaluation of the spectra. Despite some differences in the secondary amine conversions, an objective comparison of the NIR spectra, therefore, suggests that the chemical structure of the networks is similar and chemical conversion is very high. As a result, property variations can indeed be attributed to the network structure, rather than any unreacted functional groups or incomplete cure. Furthermore, given the high degree of consumption of primary and secondary amine groups, there is little evidence of significant amounts of etherification, internal cyclization, or homopolymerization in these examples.

Thermal Properties of the Epoxy Thermosets

The DSC thermograms showing the T_g endotherms after cure are shown in Figure 3(a–c) for DGEBA, DGEBF, and DGEBM, respectively. Each system reveals a single endothermic transition associated with the α type transition or T_g. For amorphous glassy network polymers, the T_g can be attributed to long-range cooperative motion of the constituent epoxy and amine segments over the entire network. No system exhibited a residual exotherm subsequent to the glass transition, indicative of complete cure and supporting the NIR results mentioned above. A preliminary

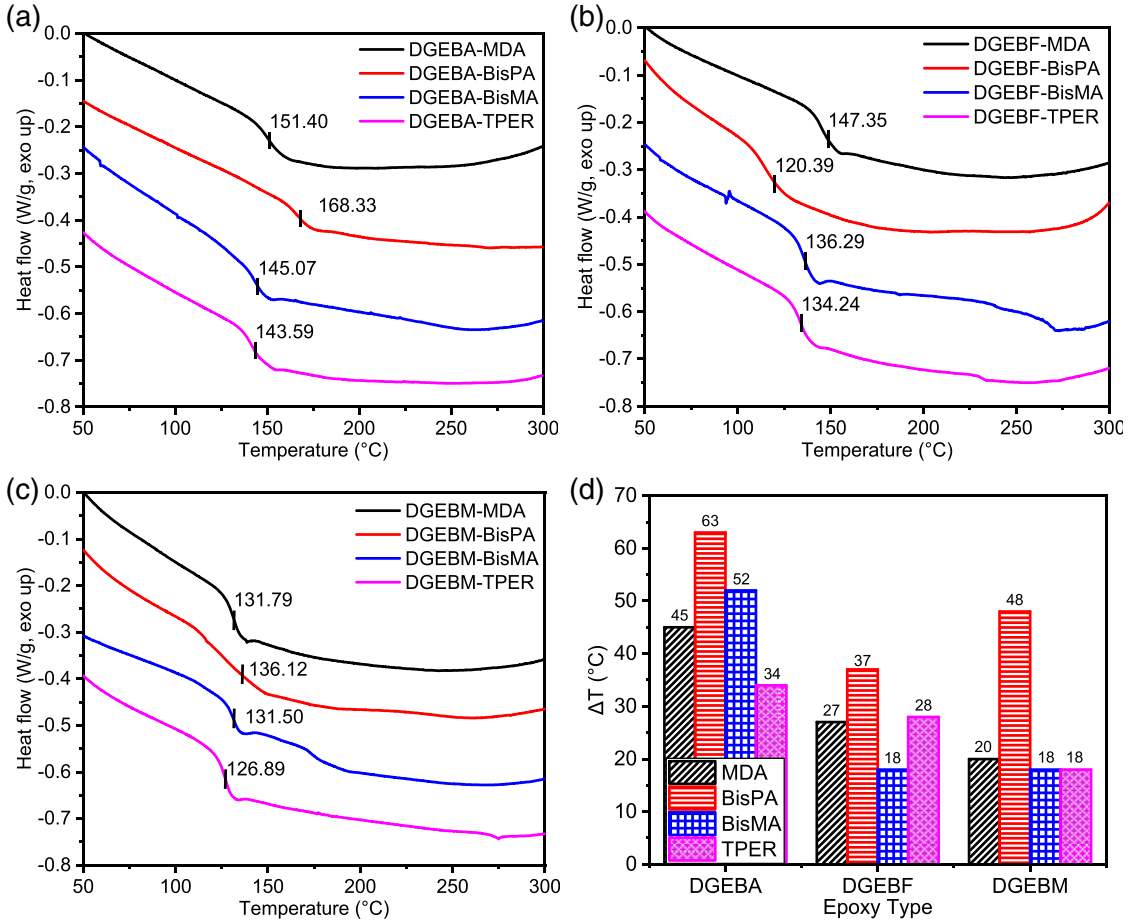

Figure 3. DSC thermograms of the cured epoxy–amine networks for (a) DGEBA, (b) DGEBF, and (c) DGEBM illustrating the lack of any residual exotherm evidence for complete cure. (d) Represents ΔT, which quantifies the breadth of the glass transition regime. [Color figure can be viewed at wileyonlinelibrary.com]

Table I. Thermal Properties Derived from DSC and DMTA

Samples	T_g (DSC) (°C)	T_g (DMTA) (°C)	CTE (ppm K^{-1})	E_{glassy} (MPa)	$E_{rubbery}$ (MPa)	ν_e (mol m^{-3})
DGEBA-MDA	151.4	160.8	73.96	1640.64	292.91	2334.69
DGEBA-BisPA	168.3	179.3	59.64	318.96	43.22	344.49
DGEBA-BisMA	145.1	154.1	73.04	335.23	40.99	326.69
DGEBA-TPE-R	143.6	151.4	67.88	311.28	45.32	361.28
DGEBF-MDA	147.4	150.8	68.54	968.70	372.01	2965.24
DGEBF-BisPA	120.4	157.4	45.78	278.09	33.86	269.911
DGEBF-BisMA	136.3	139.4	69.43	385.08	31.09	247.85
DGEBF-TPE-R	134.2	139.8	69.12	353.50	36.47	290.67
DGEBM-MDA	131.8	140.0	56.27	373.52	25.40	202.48
DGEBM-BisPA	136.1	155.1	76.58	222.29	20.14	160.53
DGEBM-BisMA	131.5	139.4	62.88	322.21	17.46	139.19
DGEBM-TPE-R	126.9	132.0	60.33	322.06	27.24	217.11

comparison of the glass transition temperatures, also shown in Table I, reveals the effect of epoxy resin on T_g is generally in the following order: DGEBA > DGEBF > DGEBM regardless of the hardener. The higher T_g for DGEBA compared to DGEBF suggests that isopropyl groups confer enhanced rigidity in the chain segment, inhibiting the polymer segments from undergoing large-scale conformational changes. Both DGEBA and DGEBF networks, however, have higher T_gs than DGEBM, which can be

directly attributed to the higher molecular weight between cross-links for DGEBM from the additional aromatic ring.

With respect to the impact of the hardener on the network T_g, the order was somewhat less systematic, but generally followed: BisPA > MDA > BisMA > TPE-R, despite the BisPA-DGEBF system displaying a particularly anomalous low result due to two overlapping endotherms at about 120 and 153 °C. The higher T_gs of the MDA and BisPA can be attributed to their rigid para substitution chain segments in contrast to the centrally meta-substituted and more flexible BisMA and TPE-R hardeners. The even lower T_g of the TPE-R cured is likely a result of the ether linkages being more flexible than isopropyl groups.[31]

Interestingly, however, there is a difference in the breadth of the glass transition endotherms as measured by the difference in temperature between the onset and offset temperature (ΔT). The results are quantified in Figure 3(d) and despite some scatter, a dependency upon the degree of para substitution within either the epoxy or the amine component of the network is again observed. The higher the level of para substitution generally revealed a wider breadth of transition compared with more meta-substituted systems, which displayed a more abrupt endothermic step. It is proposed here that since rigid polymer chains are known to have higher free volume due to poorer molecular packing, there is more local mobility or short-range motions at or near the T_g. These short-range motions may facilitate the dissipation of thermal energy over a wider temperature range and thus broaden the glass transition.[28] In contrast, the more flexible meta-substituted amines have more efficient molecular packing and reduced short-range mobility leading to a more abrupt thermal activation of the chain segments and T_g.

DMTA of the Epoxy Thermosets

The dynamic mechanical storage moduli and tan δ spectra of the networks are shown in Figure 4(a–c) for DGEBA, DGEBF, and DGEBM respectively. Each of the spectra displayed behavior typical for cured epoxy networks, consisting of a glassy elastic region prior to the glass transition temperature than a relatively stable rubbery region above T_g. During the glass transition, the storage moduli (E′) decreases exponentially in a single step decrement while the tan δ spectra exhibited a clear and mostly symmetrical peak implying a homogenous network.

Although the glassy modulus determined from DMTA can be problematic, useful trends can still be inferred and provide insights into the molecular origin of macroscale properties. From Figure 4 and Table I, the glassy moduli at 50 °C for the MDA network was significantly higher than other networks indicating reduced local mobility and lower free volume. In the case of the BisPA, BisMA, and TPE-R cured networks, the differences are more modest, although trends could still be observed. The meta-substituted BisMA and TPE-R cured networks tended to have a

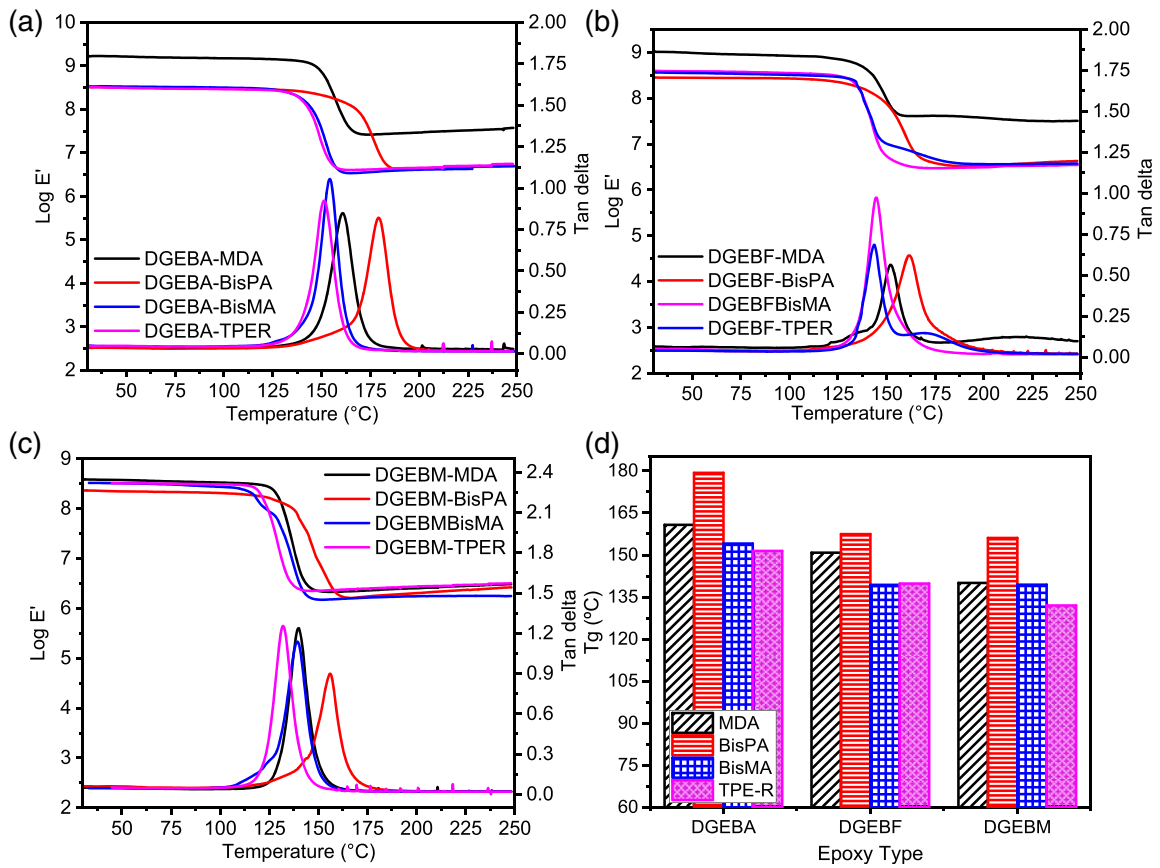

Figure 4. Dynamic mechanical thermal analysis spectra of the storage modulus (E') and tan δ after cure of the epoxy–amine networks based on (a) DGEBA, (b) DGEBF, and (c) DGEBM. Also shown is (d) a summary of the T_gs of the cured networks. [Color figure can be viewed at wileyonlinelibrary.com]

higher storage modulus compared with the para-substituted BisPA for the DGEBF and DGEBM networks supporting the hypothesis that meta-substitution increases modulus through reduced free volume and better equilibrium packing.[17] The glassy modulus for the DGEBA networks appeared comparatively similar regardless of tri-aryl amine hardener.

The crosslink densities calculated using eq. (1) shown in Table I again follow quite consistent trends. With respect to the different epoxy resins, crosslink density exhibits a decreasing trend from DGEBA to DGEBF and finally to DGEBM which has the lowest value. Although it is not surprising that the DGEBM epoxy resin has the lowest crosslink density, it is interesting to note that the presence of the isopropyl groups increases crosslink density complementing the higher T_gs measured for DGEBA from DMTA and DSC. With respect to the amine hardeners, the bi-aryl MDA networks cured with DGEBA and DGEBF in particular have by far the highest crosslink densities due to its lower molecular weight between crosslinks compared with the tri-aryl amine networks. Considering the impact of the tri-aryl amines, although somewhat varied, a modest trend can be observed with the crosslink density of the TPE-R generally being a little higher than the relatively similar BisPA and BisMA amines.

Regardless of the amine, the DGEBA networks exhibited the highest T_gs, followed by DGEBF and then DGEBM, supporting the crosslink density calculations in Table I and the higher rigidity of the isopropyl groups. With respect to the amine hardeners, however, the network with the highest crosslink density, MDA, did not, in fact, display the highest T_g, being lower than the para-substituted BisPA networks. The BisMA and TPE-R networks were both significantly lower than BisPA due to their meta-substituted structures again providing enhanced flexibility, particularly for the ether linkage in TPE-R.[31] Given that the epoxy–amine networks in this study have been shown to be fully cured using NIR, the changes in T_g can be unambiguously ascribed to variations in the molecular structure. Indeed, it is important to remember that DGEBA and DGEBF themselves are all para-substituted compared with DGEBM, which has two para-substituted outer aromatic rings and a meta-substituted central para aromatic ring. Although the lower T_g of the DGEBM networks is to be expected, T_g is clearly not completely controlled by the molecular weight between crosslinks since the BisMA and BisPA networks have the same chemical structure and different T_g. Furthermore, networks cured with MDA had higher calculated crosslink densities, yet lower T_g's than any of the tri-aryl BisPA networks. Indeed, the networks that exhibited the highest T_g were the DGEBA-BisPA (179 °C), followed by DGEBF-BisPA (162 °C) and finally the DGEBM-BisPA (156 °C), which is based upon a tri-aryl amine and epoxy resin. Clearly, therefore, the aromatic substitution pattern on the backbone has a significant effect. Para substitution patterns allow the phenyl ring to rotate as shown in Figure 5, which acts as an energy dissipation mechanism that increases the energy required to initiate cooperative segmental motion hence increasing T_g. It is proposed that the isopropyl groups in the tri-aryl amines must provide some additional rotational ability, which may cumulatively add to the energy dissipating mechanism leading to an even higher T_g.[27] The BisPA hardener, therefore would benefit from both the rotational ability of an all para tri-aryl backbone and two additional isopropyl moieties. The increase in T_g likely results from the additional energy required to initiate segmental cooperative motion of tri-aryl structural segments rather than bi-aryl segments. Interestingly though, the centrally meta-substituted amine cured networks, BisMA and TPE-R, did not have the same effect as the para-substituted BisPA hardener. Meta-substitution has been shown to not undergo phenylene rotation or π flips due to the absence of the axis of rotation, reducing the spontaneous energy dissipating mechanism and hence reducing T_g.[27,28] This lack of rotation caused by meta-substitution provides further reinforcement and higher modulus but lowers the energy required to initiate cooperative segmental motion of the crosslinks.

Thermomechanical Analysis of the Epoxy Thermosets

TMA was used to determine the thermal expansion characteristics of the epoxy networks below the network T_g as shown in Figure 6. The glassy CTE showed that the DGEBA-based networks tended to exhibit the highest CTE apart from the unusually low DGEBA-BisPA network. This can be attributed to higher chain rigidity, which can be defined as the resistance of the polymer chain to undergo long-range and cooperative conformational

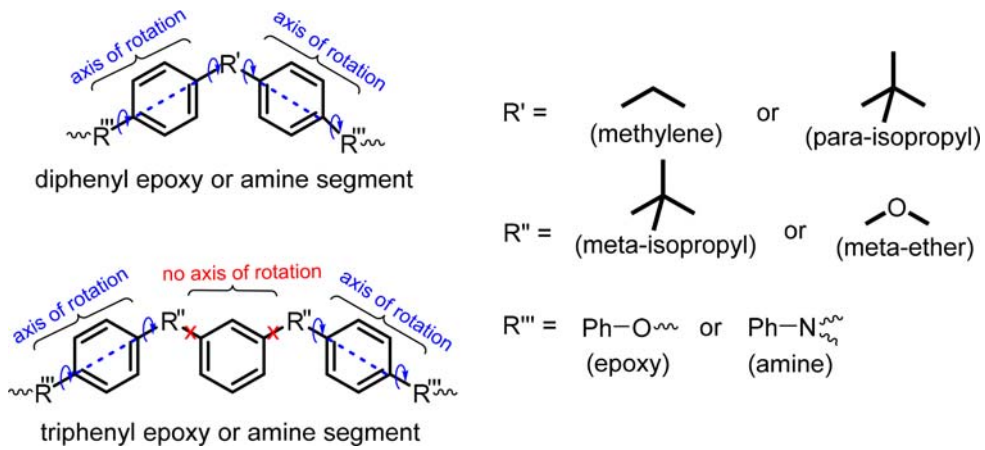

Figure 5. Comparison of the local rotational mobility of epoxy or amine segments for both the bi- and tri-aryl structures within the cured network in the case of para- and meta-substituted structures. [Color figure can be viewed at wileyonlinelibrary.com]

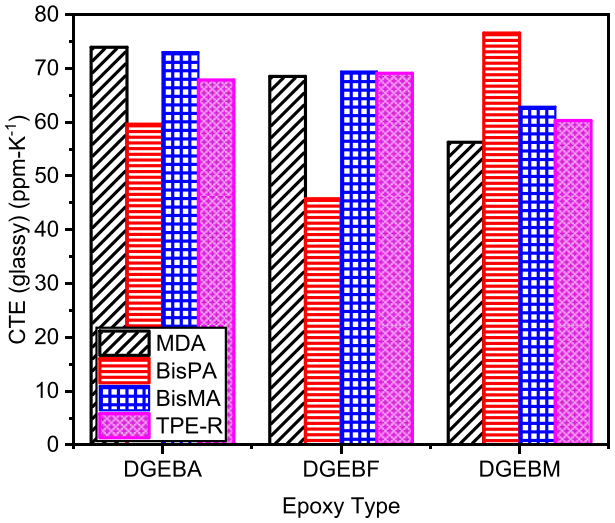

Figure 6. Coefficients of thermal expansion of the epoxy–amine networks in the glassy state. [Color figure can be viewed at wileyonlinelibrary.com]

changes when energy is supplied to the system.[28] As a result, the rigid polymer chains cannot pack efficiently resulting in a higher free volume in the cured network, resulting in a greater release of stress and hence thermal expansion when heated.[17] Although modest, the lower CTE for the DGEBF and DGEBM networks can be attributed to greater conformational freedom to pack more efficiently that releases less stress during heating. An additional factor with the DGEBM, which might influence CTE, is that it is a nonsymmetric meta-substituted epoxy resin homologous to DGEBA having phenyl rings linked by isopropyl groups. These groups may increase steric hindrances below the T_g resulting in resistance to volumetric expansion during heating.[32]

Compressive Properties of the Epoxy Thermosets

Under compressive loading shown in Figure 7(a–c), all of the epoxy networks exhibited somewhat ductile behavior, exhibiting yielding at strains of more than 10% and fracture at strains more than 45%. The stress versus strain data shows that an elastic regime (<5% strain) occurred followed by yielding, strain hardening and then further hardening until failure. Post-yield, the polymer chains in the network undergo reorientation resulting in less molecular interaction prior to catastrophic failure. Closer examination of each stress versus strain plot for the DGEBA, DGEBF, and DGEBM networks, reveals a modest increase in strain-softening by the DGEBF and DGEBM resins compared with DGEBA. This can be attributed due to an increased rigidity and reduced molecular mobility of the isopropyl containing DGEBA networks.[27–29]

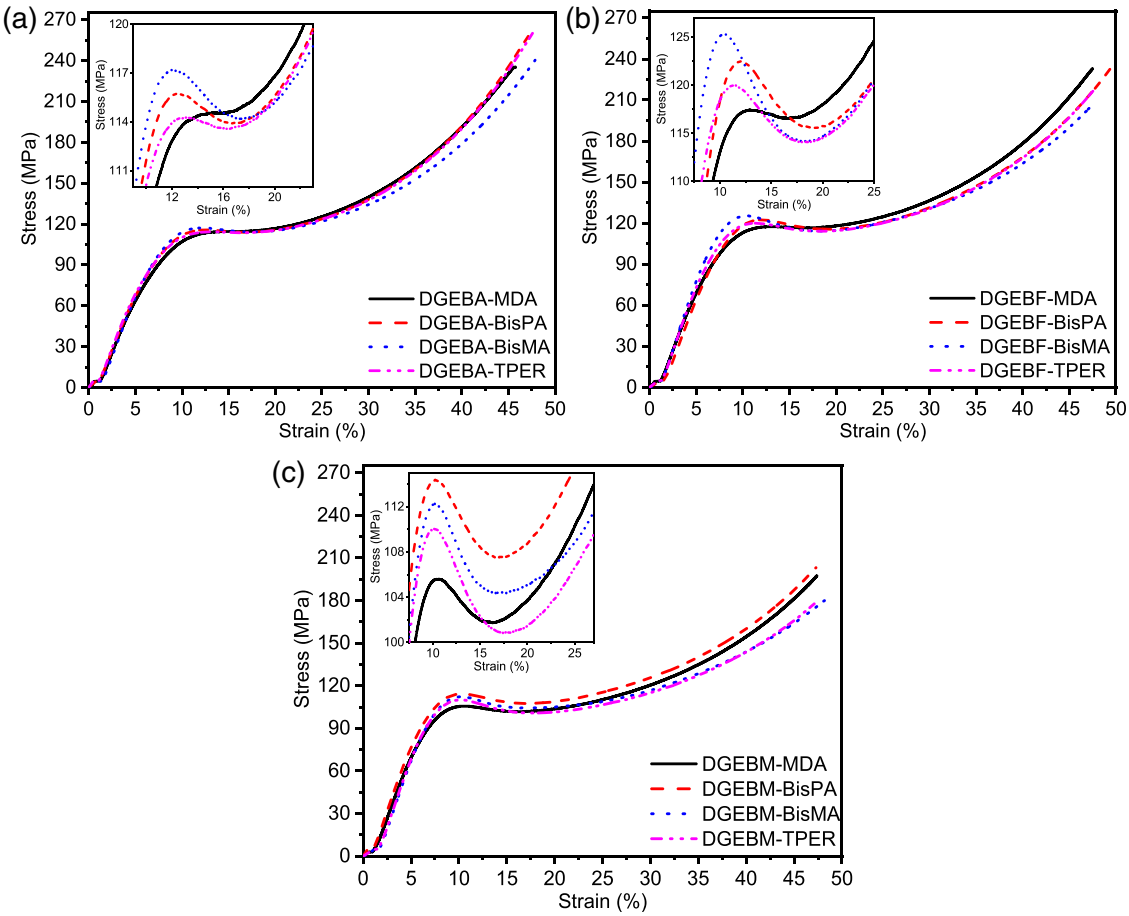

Figure 7. Stress–strain curves of the epoxy–amine networks based on (a) DGEBA, (b) DGEBF, and DGEBM epoxy resins. [Color figure can be viewed at wileyonlinelibrary.com]

Closer examination of the effect of the amines from the insets in Figure 7(a–c) shows there is an increase in the maximum yield stress and a reduction in degree of strain-softening, regardless of the epoxy resin, in order of BisPA ~ BisMA > TPE-R > MDA. This is despite the yield strains not changing noticeably and highlights the increased stress required to initiate longer-range cooperative motion of the tri-aryl networks compared with the bi-aryl MDA networks. Furthermore, the tri-aryl isopropyl networks based upon BisPA and BisMA both had higher yield stress than the TPE-R networks regardless of epoxy resin. This likely reflects an increased mobility of the ether linkages compared with the isopropyl groups that allow for greater molecular rearrangement or relaxation during yield and hence lower stress levels.[27,33]

The compressive modulus, strength, and yield strain are shown in Figure 8(a–c), respectively. For the modulus, the DGEBA networks generally have the lowest values, followed by DGEBF and then DGEBM. With respect to the hardeners, the tri-aryl amines all increased the modulus compared with the bi-aryl MDA, with the meta-substituted BisMA increasing modulus the most, followed by TPE-R and the least improvement being BisPA. All of these variations can be explained in relation to the restricted phenylene ring rotation in the glassy state providing molecular reinforcement or anti-plasticization and an improved equilibrium packing density leading to a lower free volume.[5,17]

For the yield strengths, the DGEBF networks have the lowest values, followed by DGEBA and then the DGEBM, which has the highest. This can be attributed to the higher forces required to initiate long-range cooperative motion of a crosslinked network as discussed earlier. The isopropyl groups again impart rigidity compared with the methylene linkages of the DGEBF, while the additional isopropyl aromatic group in DGEBM increases strength by further restricting longer-range cooperative motion. In comparison, the bi-aryl MDA cured network has lower strength than all of the tri-aryl amine networks. The effect of the tri-aryl amines on the strength was opposite to that of the modulus, decreasing from BisPA to BisMA and TPE-R as shown in Figure 8(b). Clearly, rigid rather than flexible substructures are more beneficial to increased strength.

The yield strain is shown in Figure 8(c) displays different behavior again, this time decreasing in order of DGEBA, DGEBF, and finally DGEBM, again suggesting that chain rigidity is paramount in determining the yield strain. As a function of amine, the more rigid, the higher the yield strain. As can be seen, MDA and BisPA were similarly high regardless of epoxy resin, while the flexible BisMA and TPE-R amines imparted the lowest yield strains.

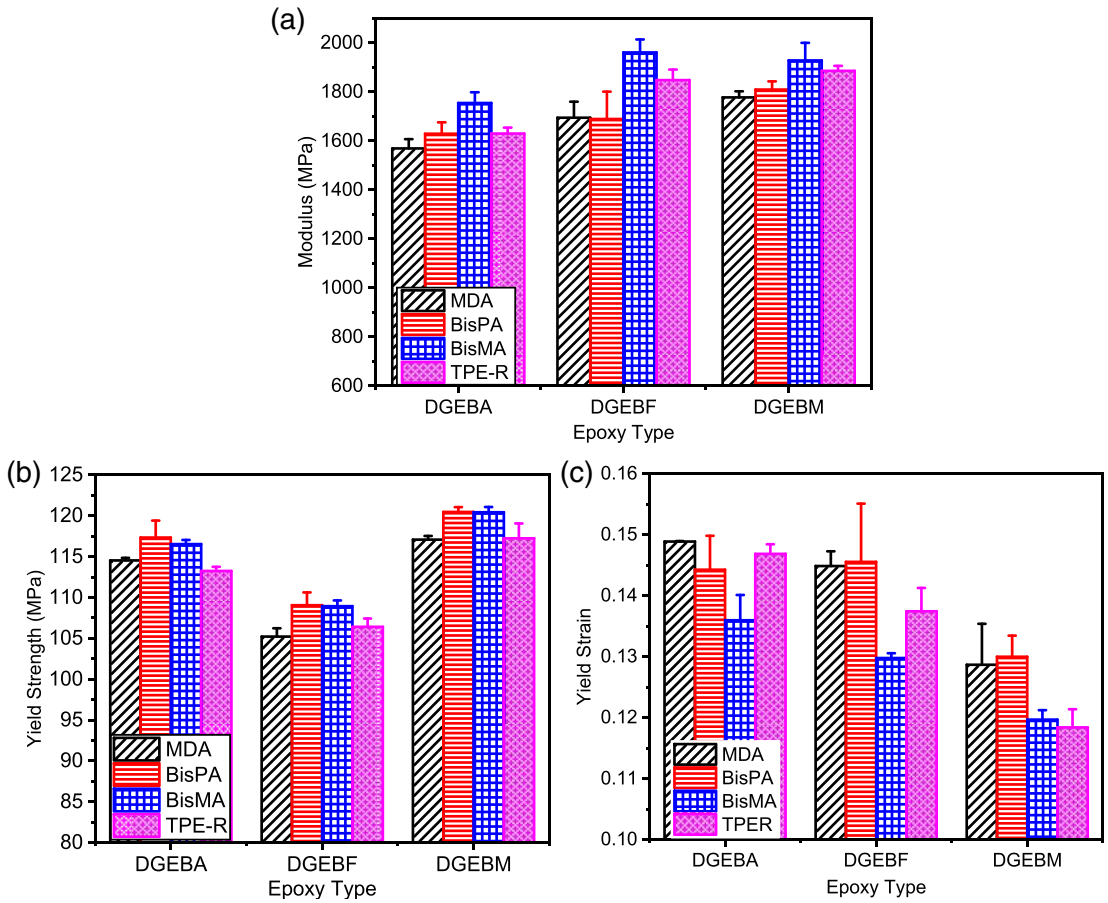

Figure 8. Compressive (a) modulus, (b) yield strength, and (c) yield strain properties of the cured epoxy–amine networks. [Color figure can be viewed at wileyonlinelibrary.com]

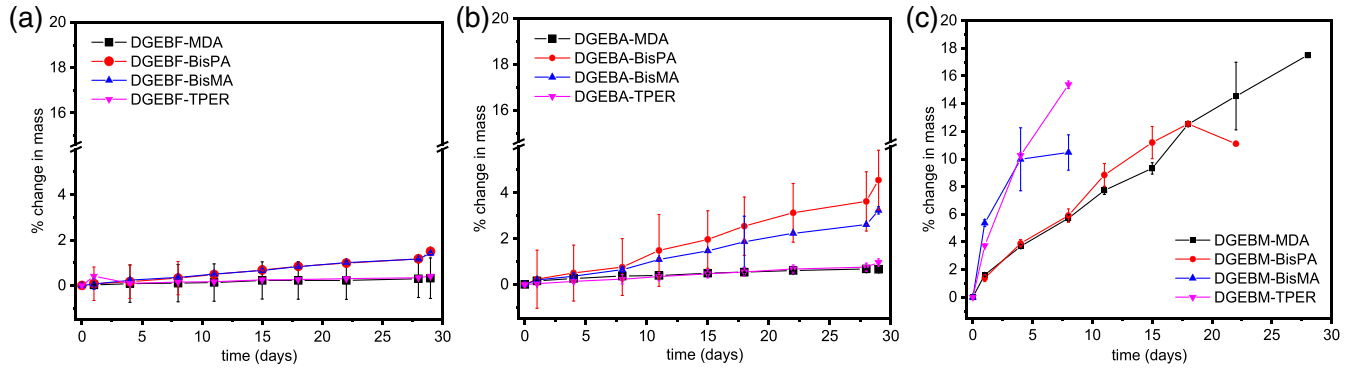

Figure 9. MEK ingress as a function of time for the (a) DGEBF, (b) DGEBA, and DGEBM cured networks. [Color figure can be viewed at wileyonlinelibrary.com]

MEK Resistance of the Epoxy Thermosets

Resistance to solvent ingress such as MEK is a critical requirement for any high-performance epoxy network and composites. In the present study, the epoxy networks were immersed in MEK at room temperature and ingress monitored over the course of 4 weeks. The resultant changes in mass are shown in Figure 9(a–c) for the DGEBA, DGEBF, and DGEBM networks. As can be clearly seen from the plots, the DGEBF networks are significantly more resistant to MEK ingress compared with DGEBA. After 28 days, the mass of the DGEBF networks has increased by an average of 0.32, 1.50, 1.42, and 0.41% cured with MDA, BisPA, BisMA, and TPE-R, respectively, while the DGEBA networks mass increased by a corresponding 0.66, 4.56, 3.23, and 0.97% cured with MDA, BisPA, BisMA, and TPE-R, respectively. The DGEBM networks displayed very poor behavior increasing in mass by at least 10% over this time, with the BisMA and TPE-R networks essentially dissolving in MEK only after 10 days.

With respect to the impact of the amines, the MDA displayed the greatest resistance to MEK ingress overall, although, for the DGEBA and DGEBGF networks, the TPE-R cured networks showed similar MEK resistance. The DGEBM networks had extremely poor MEK resistance for all of the networks making it difficult to relate the observed changes to network structure. However, for the DGEBA and DGEBF networks, it was clear that the MDA and TPE-R networks had superior MEK resistance compared with the BisMA and BisPA networks after 28 days soaking.

The MEK ingress has been observed to be affected by several different network parameters such as crosslink, free volume hole size (V_h), and fractional free volume. MEK is a good solvent for multi-aryl compounds having a hydrodynamic volume of 81 Å^3, and resins with V_h of around 61 Å^3 prevent the solvent ingress.[34] Effect of aromatic substitution on the cure reaction and network properties of anhydride cured triphenyl ether tetraglycidyl epoxy resins. And so, the MEK ingress test will give an idea about the average hole volume size (V_h) of the polymer network that is formed after cure. Frank *et al.* showed that the solvent ingress could be used to gain insight into the free volume of the network. Using the hydrodynamic volume of MEK as 63 Å^3, if the free volume voids are larger than 63 Å^3, MEK can be absorbed, but much less so if the voids are smaller.

CONCLUSIONS

Three different epoxy resins have been cured with a series of bi- and tri-aryl amines to systematically explore their structure–property relationships after cure. The research focused on the effect of changing (1) the aromatic linkages from methylene to isopropyl within an epoxy resin, (2) the substitution pattern within the central aromatic rings of the amine hardeners from meta to para, (3) the meta-substituted aromatic linkage of the central aromatic ring from isopropyl to ether, and (4) the number of aromatic rings from 2 to 3 in either the epoxy or amine.

Isopropyl versus methylene linkages in the epoxy resin increased T_g, yield strength, yield strain, CTE, and MEK ingress while reducing modulus. These changes were described in terms of the isopropyl group increasing stiffness, reducing short-range molecular mobility and cooperative segmental motion, and reducing packing efficiency.

Varying substitution of the central aromatic group in the amine from meta to para increased T_g, left yield strength unaffected, increased yield strain while reducing modulus, and left CTE and MEK ingress unaffected. In addition to the increased molecular rigidity reducing packing efficiency and short-range molecular mobility, the increased phenylene rotations provided additional energy dissipation mechanisms, which increased T_g and strain yield.

Varying the meta-substituted aromatic linkages in the amines from isopropyl to ether reduced T_g, strength and modulus, left MEK unaffected while increasing yield strain. These changes were described in terms of the enhanced flexibility of the ether linkages.

Increasing the aromatic rings in the epoxy reduced T_g, CTE, and yield strain, while increasing modulus, strength, and MEK ingress. Increasing the aromatic rings from 2 to 3, reduced crosslinked density and also aided packing efficiency.

ACKNOWLEDGMENTS

Russell J. Varley gratefully acknowledges initial funding from the Boeing Company. This work was partially supported by The Australian Research Council (DP180100094) and The Office of Naval Research Global (N62909-18-1-2024).

REFERENCES

1. Ellis, B. Chemistry and Technology of Epoxy Resins. 1st ed.; Springer Netherlands: Dordrecht, **1993**.
2. Ashcroft, W. R. *Three Bond Tech. News*. **1990**, *32*, 1.
3. Vidil, T.; Tournilhac, F.; Musso, S.; Robisson, A.; Leibler, L. *Prog. Polym. Sci.* **2016**, *62*, 126.
4. Strong, A. B. Fundamentals of Composites Manufacturing: Materials, Methods, and Applications. Vol. *3*. 2nd ed.; Society of Manufacturing Engineers: Dearborn, Michigan, **1992**.
5. Frank, K.; Childers, C.; Dutta, D.; Gidley, D.; Jackson, M.; Ward, S.; Maskell, R.; Wiggins, J. *Polymer*. **2013**, *54*, 403.
6. Jin, F. L.; Li, X.; Park, S. J. *J. Ind. Eng. Chem.* **2015**, *29*, 1.
7. Jagadeesh, K. S.; Shashikiran, K. *J. Appl. Polym. Sci.* **2004**, *93*, 2790.
8. Zheng, F.; Zhao, X.; Yang, X.; Zhang, Y.; Huang, W. *J. Appl. Polym. Sci.* **2014**, *131*, 1.
9. Liu, T.; Zhang, L.; Chen, R.; Wang, L.; Han, B.; Meng, Y.; Li, X. *Ind. Eng. Chem. Res.* **2017**, *56*, 7708.
10. Duann, Y. F.; Liu, T. M.; Cheng, K. C.; Su, W. F. *Polym. Degrad. Stab.* **2004**, *84*, 305.
11. Harada, M.; Morioka, D.; Ochi, M. *J. Appl. Polym. Sci.* **2018**, *135*, 1.
12. Arita, K.; Oyama, T. *J. Appl. Polym. Sci.* **2016**, *133*, 1.
13. Wang, P.; Yang, F.; Li, L.; Cai, Z. *Polym. Degrad. Stab.* **2016**, *129*, 156.
14. Park, H.; Kim, B.; Choi, J.; Cho, M. *Polymer*. **2018**, *136*, 128.
15. Chiu, Y. C.; Huang, C. C.; Tsai, H. C.; Prasannan, A.; Toyoko, I. *Polym. Bull.* **2013**, *70*, 1367.
16. Wang, H.; Zhang, Y.; Zhu, L.; Du, Z.; Zhang, B.; Zhang, Y. *Thermochim. Acta*. **2011**, *521*, 18.
17. Ramsdale-Capper, R.; Foreman, J. P. *Polymer*. **2018**, *146*, 321.
18. Nakka, J. S.; Jansen, K. M. B.; Ernst, L. J. *J. Polym. Res.* **2011**, *18*, 1879.
19. Wan, J.; Li, C.; Bu, Z.-Y.; Xu, C.-J.; Li, B.-G.; Fan, H. *Chem. Eng. J.* **2012**, *188*, 160.
20. Liu, H.; Uhlherr, A.; Varley, R. J.; Bannister, M. K. *J. Polym. Sci., Part A: Polym. Chem.* **2004**, *42*, 3143.
21. Vogel, W.; Dingemans, T. J.; Varley, R. J.; Tian, W.; Dao, B.; Tucker, S. J.; Christensen, S. *High Perform. Polym.* **2014**, *26*, 420.
22. Tucker, S. J. Ph.D. Thesis, The University of Southern Mississippi, **2010**.
23. Jin, Q.; Misasi, J. M.; Wiggins, J. S.; Morgan, S. E. *Polymer*. **2015**, *73*, 174.
24. Fei, X.; Wei, W.; Tang, Y.; Zhu, Y.; Luo, J.; Chen, M.; Liu, X. *Eur. Polym. J.* **2017**, *90*, 431.
25. Strzelec, K.; Baczek, N.; Ostrowska, S.; Wąsikowska, K.; Szynkowska, M. I.; Grams, J. *C. R. Chim.* **2012**, *15*, 1065.
26. Zhang, Y.; Shang, C.; Yang, X.; Zhao, X.; Huang, W. *J. Mater. Sci.* **2012**, *47*, 4415.
27. Tu, J.; Tucker, S. J.; Christensen, S.; Sayed, A. R.; Jarrett, W. L.; Wiggins, J. S. *Macromolecules*. **2015**, *48*, 1748.
28. Heinz, S.; Tu, J.; Jackson, M.; Wiggins, J. *Polymer*. **2016**, *82*, 87.
29. Varley, R. J.; Dao, B.; Tucker, S.; Christensen, S.; Wiggins, J.; Dingemans, T.; Vogel, W.; Marchetti, M.; Madzarevic, Z. *J. Appl. Polym. Sci.* **2019**, *136*, 47383.
30. Flory, P. J. Principles of Polymer Chemistry. 1st ed.; Cornell University Press: Ithaca, **1953**.
31. Misasi, J. Ph.D. Thesis, The University of Southern Mississippi, **2015**.
32. Dong, K.; Zhang, J.; Cao, M.; Wang, M.; Gu, B.; Sun, B. *Polym. Test.* **2016**, *55*, 44.
33. Wu, J.; Xiao, C.; Yee, A. F.; Klug, C. A.; Schaefer, J. *J. Polym. Sci., Part B: Polym. Phys.* **2001**, *39*, 1730.
34. Jackson, M.; Kaushik, M.; Nazarenko, S.; Ward, S.; Maskell, R.; Wiggins, J. *Polymer*. **2011**, *52*, 4528.